



Hollow microneedle-mediated intradermal delivery of model vaccine antigen-loaded PLGA nanoparticles elicits protective T cell-mediated immunity to an intracellular bacterium



Anne Marit de Groot^{a,1}, Guangsheng Du^{b,1}, Juha Mönkäre^b, Anouk C.M. Platteel^a, Femke Broere^a, Joke A. Bouwstra^b, Alice J.A.M. Sijts^{a,*}

^a Department of Infectious diseases and Immunology, Faculty of Veterinary Medicine, Utrecht University, Utrecht, The Netherlands

^b Division of Drug Delivery Technology, Cluster Bio-Therapeutics, Leiden Academic Centre for Drug Research, Leiden University, Leiden, The Netherlands

ARTICLE INFO

Keywords:

Protein vaccine
Hollow microneedles
Intradermal immunization
PLGA nanoparticles
Cytotoxic T cell response

ABSTRACT

The skin is an attractive organ for immunization due to the presence of a large number of epidermal and dermal antigen-presenting cells. Hollow microneedles allow for precise and non-invasive intradermal delivery of vaccines. In this study, ovalbumin (OVA)-loaded poly(lactic-co-glycolic acid) (PLGA) nanoparticles with and without TLR3 agonist poly(I:C) were prepared and administered intradermally by hollow microneedles. The capacity of the PLGA nanoparticles to induce a cytotoxic T cell response, contributing to protection against intracellular pathogens, was examined. We show that a single injection of OVA-loaded PLGA nanoparticles, compared to soluble OVA, primed both adoptively transferred antigen-specific naïve transgenic CD8⁺ and CD4⁺ T cells with markedly high efficiency. Applying a triple immunization protocol, PLGA nanoparticles primed also endogenous OVA-specific CD8⁺ T cells. Immune response, following immunization with in particular anionic PLGA nanoparticles co-encapsulated with OVA and poly(I:C), provided protection against a recombinant strain of the intracellular bacterium *Listeria monocytogenes*, secreting OVA. Taken together, we show that PLGA nanoparticle formulation is an excellent delivery system for protein antigen into the skin and that protective cellular immune responses can be induced using hollow microneedles for intradermal immunizations.

1. Introduction

The skin is an organ with many immune cells and is considered a potent organ for immunizations [1]. However, the challenge is to deliver high-molecular-weight antigens across the stratum corneum, which is the outermost layer of the skin and acts as an effective natural barrier for penetration of pathogens and allergens into the skin. One of the methods to circumvent the skin barrier is the use of microneedles. Microneedles are miniaturized needles that provide the possibility of minimally invasive vaccination in the dermis and epidermis of the skin. There are other benefits in using microneedles compared to traditional hypodermic needles, like possible painless vaccination, the requirement of less trained personnel and reduced contamination risk [2]. Nowadays a wide variety of these microneedles exist, including solid, coated, dissolving and hollow microneedles [3,4].

Hollow microneedles have multiple benefits, for instance they can be used to inject a wide variety of fluids into the skin at different pressure-driven flow rates [3,5,6] and offer the highest precision in

dose delivery among all microneedle types. Furthermore, they offer the possibility to screen formulations without time-consuming design and preparation of microneedles, as in case of coated and dissolving microneedles. Recently, hollow microneedles and an applicator for them were developed in our laboratory to inject formulations in precise manner into the skin. These microneedles were successfully used for formulations with inactivated polio virus vaccine in rats resulting in effective humoral immune responses [7–9]. However, whether hollow microneedle-mediated delivery may also induce CD8⁺ T cell responses towards vaccine antigens is presently unclear.

Cytotoxic CD8⁺ T cells play an important role in cellular immune protection against intracellular pathogens or tumor growth. To induce such CD8⁺ T cell responses, an antigen needs to be processed in the cell and presented by MHC-I molecules on professional antigen-presenting cells (pAPC) to the immune system. Delivery of vaccine protein antigens over the cellular membrane can be achieved using delivery systems and over the past decades different types of them, such as polymeric nanoparticles, emulsions and lipid-based nanoparticles have been

* Corresponding author at: Utrecht University, Yalelaan 1, 3584CL Utrecht, The Netherlands.

E-mail address: e.j.a.m.sijts@uu.nl (A.J.A.M. Sijts).

¹ Equal contributions.

developed [10–12]. Nano-encapsulation of antigens has several advantages, such as stabilization of antigens *in vivo*, enhancement of the uptake by pAPC and also reduction of antigen release into systemic circulation [4,13]. The immune outcome can be potentially shaped by using nanoparticles with difference size [14] and surface charge [15], and by co-encapsulating antigen and adjuvant into the nanoparticles [16,17].

For the production of polymeric nanoparticles, poly(lactic-co-glycolic acid) (PLGA) is the most commonly used polymer, because of its superior biocompatibility and biodegradability [18–20]. Previous studies have shown that model antigen- and adjuvant-loaded PLGA nanoparticles used for vaccination were able to improve the induction of cell-mediated immune response in mice [17,21–23]. However, relatively little is known about how encapsulation in PLGA nanoparticles modifies T cell responses to antigen/adjuvant combinations that are delivered intradermally by different novel types of microneedles. One recent study reported that PLGA nanoparticles, delivered intradermally using dissolving microneedles arrays [24], induced cellular immune responses and protection against viral infection and tumor growth.

In this study, nanoparticles were prepared and characterized in terms of size, surface charge and antigen/adjuvant release profiles. We investigated the ability of hollow microneedle-delivered protein antigens, encapsulated in either anionic or cationic PLGA nanoparticles without and with co-encapsulated TLR 3 agonist poly(I:C) to induce a protective, cellular immune response towards an intracellular pathogen in a mouse model.

2. Materials and methods

2.1. Materials

PLGA (acid terminated, lactide glycolide 50:50, Mw 24,000–38,000), polyethylenimine (PEI, linear, average M_n 10,000), Roswell Park Memorial Institute medium (RPMI) and Fetal bovine serum (FBS) were purchased from Sigma-Aldrich (Zwijndrecht, The Netherlands). PVA 4–88 (31 kDa) was obtained from Fluka (Steinheim, Germany). Endotoxin-free ovalbumin (OVA), polyinosinic-polycytidylic acid (poly(I:C)) (low molecular weight) and its rhodamine-labelled version were obtained from Invivogen (Toulouse, France). Alexa647 labelled OVA (OVA-Alexa647) was ordered from Thermo-Fischer Scientific (Waltham, MA). Dimethylsulfoxide (DMSO) was obtained from Biosolve BV (Valkenswaard, The Netherlands). Sodium dodecyl sulfate (SDS) was obtained from Merck Millipore (Hohenbrunn, Germany). Ammonium-Chloride-Potassium (ACK) lysis buffer (150 mM NH_4Cl , 1 mM NaHCO_3 ; pH 7.40) and 1 mM phosphate buffer (PB; pH 7.4) were prepared in the lab. Milli-Q water (18.2 $\text{M}\Omega/\text{cm}$, Millipore Co., USA) was used for the preparation of solutions. Sterile phosphate buffered saline (PBS) was obtained from Braun (Oss, The Netherlands). All other chemicals used are of analytical grade.

Purification antibodies used for DynaBeads® selection were all made in house and included the following antibody clones: αCD11b (clone M1/70), $\alpha\text{MHC-II}$ (M5/114), αB220 (RA3-6B2), αCD4 (GK1.4), αCD8 (YTS169) and αCD25 (PC61). Purification antibodies for sorting via flow cytometry were $\alpha\text{CD8-APC}$ (53-6.7; eBioscience), CD44-FITC (IM7; eBioscience) and CD62L-PE (MEL-14; BD Bioscience) using a BD influx (BD Biosciences). For the detection of the adoptively transferred T cells the antibodies $\alpha\text{CD45.2-PerCpCy5.5}$ (104; eBioscience), $\alpha\text{CD4-PE}$ (GK1.5; eBioscience) and $\alpha\text{CD8-APC}$ (53-6.7; BD Bioscience) were used. Detection of the endogenous T cells was measured using the antibodies $\alpha\text{CD8-APC}$ (53-6.7; eBioscience), $\alpha\text{CD4-eFluor450}$ (GK1.5; eBioscience), $\alpha\text{CD62L-Horizon B510}$ or $\alpha\text{CD44-FITC}$ (IM7; eBioscience), $\alpha\text{CD16/CD32-unstained}$ (2.4G2; made in house) and $\alpha\text{IFN}\gamma\text{-PE}$ (XMG1.2; eBioscience).

2.2. Preparation of PLGA nanoparticles

OVA-loaded PLGA nanoparticles were prepared by double emulsion with solvent evaporation method as previously reported with modifications [25]. Briefly, 75 μl OVA (20 mg/ml) in PBS was dispersed in 1 ml PLGA (25 mg/ml) in ethyl acetate by a Branson sonifier 250 (Danbury, USA) for 15 s with a power of 20 W. To prepare anionic OVA-loaded PLGA nanoparticles (anPLGA-OVA), the obtained water-in-oil emulsion was emulsified with 2 ml 2% (w/v) PVA with the sonifier (15 s, 20 W) to get a water-in-oil-in-water double emulsion. In case of cationic OVA-loaded PLGA nanoparticles (catPLGA-OVA), the single emulsion was emulsified with 2 ml 2% (w/v) PVA and 4% (w/v) PEI solution. The double emulsion was added dropwise into 25 ml 0.3% (w/v) PVA (40 °C) under stirring. The ethyl acetate was evaporated by a rotary evaporator (Buchi rotavapor R210, Switzerland) for 3 h (150 mbar, 40 °C). The nanoparticle suspension was centrifugated (Avanti™ J-20XP centrifuge, Beckman Coulter, Brea, CA) at 35000 g for 10 min, washed twice with 1 mM PB to remove the excess OVA and PVA, and dried in an Alpha-1-2 freeze dryer (Osterode, Germany, –49 °C, 90 mbar) overnight. To prepare OVA and poly(I:C) co-encapsulated PLGA nanoparticles (anPLGA-OVA-PIC), 18.75 μl OVA (40 mg/ml) and 75 μl poly(I:C) (46.7 mg/ml, including 0.03% fluorescently labelled equivalent) were emulsified with 1 ml PLGA (25 mg/ml) in ethyl acetate to obtain the water-in-oil emulsion. The remaining of the procedure was identical to that of anPLGA-OVA. The obtained nanoparticles were stored at 4 °C for analysis and further use. To prepare the PLGA nanoparticles for release study, 10% of total OVA was replaced with OVA-Alexa647 the preparation.

2.3. Characterization of PLGA nanoparticles

The size (Z-average) and polydispersity index (PDI) of nanoparticles were measured by dynamic light scattering and the zeta potential of nanoparticles was measured by laser doppler velocimetry using a Nano ZS® zetasizer (Malvern Instruments, Worcestershire, U.K.). The samples were diluted with 1 mM PB buffer to a nanoparticle concentration of 25 $\mu\text{g}/\text{ml}$ before each measurement. To determine the loading efficiency of OVA and poly(I:C) in PLGA nanoparticles, approximately 1 mg of nanoparticles were dissolved in a mixture of 15% (v/v) DMSO and 85% (v/v) 0.05 M NaOH and 0.5% SDS. The amount of OVA was determined by MicroBCA method following the manufacturer's instructions. The amount of poly(I:C) was quantified by the fluorescence intensity of rhodamine labelled poly(I:C) (λ_{ex} 545 nm/ λ_{em} 576 nm). The encapsulation efficiency (EE) and loading capacity (LC) of OVA and poly(I:C) in the nanoparticles were calculated as below:

$$\text{EE}\% = \frac{M_{\text{loaded OVA/poly(I:C)}}}{M_{\text{total ova/poly(I:C)}}} \times 100\% \quad (1)$$

$$\text{LC}\% = \frac{M_{\text{loaded OVA/poly(I:C)}}}{M_{\text{nanoparticles}}} \times 100\% \quad (2)$$

where $M_{\text{loaded OVA/poly(I:C)}}$ represents the mass of loaded OVA or poly(I:C), $M_{\text{total OVA/poly(I:C)}}$ is the total amount of OVA or poly(I:C) added to the formulation and $M_{\text{nanoparticles}}$ is the weight of nanoparticles.

2.4. Release of OVA and poly(I:C) from PLGA nanoparticles

Nanoparticles were prepared in triplicate as described above. To study the release of OVA and poly(I:C) from PLGA nanoparticles, 3 mg anPLGA-OVA, catPLGA-OVA or anPLGA-OVA-PIC were dispersed into 1 ml RPMI supplemented with 10% FBS and incubated at 37 °C with a shaking speed of 350 rpm. At different time points, the suspensions were centrifugated (9000g, 5 min) with Sigma 1–15 centrifuge (Osterode, Germany). A release sample of 600 μl of the supernatant was collected and replaced by fresh medium. The released amount of OVA and poly(I:C) was determined by fluorescence intensity of OVA-

Alexa647 (λ_{ex} 647 nm/ λ_{em} 671 nm) and rhodamine labelled poly(I:C) (λ_{ex} 545 nm/ λ_{em} 576 nm), respectively.

2.5. Mice and intradermal immunizations

8–18 week old male B6-SJL/ptprcaPep3b/BoyCrl (B6-SJL) wild type mice and 8–30 week old transgenic (tg) mice that express pOVA_{323–339}-specific T cell receptor (OT-II mice) or pOVA_{257–264}-specific T cell receptor (OT-I mice) were initially obtained from Charles River and were bred in house. Abdomen of mice were shaved prior to immunization on both flanks and intradermal immunization was done using a single hollow microneedle as reported previously [8,9]. The hollow microneedle was inserted into the abdomen of mice using an applicator controlling precisely the depth, volume and rate of the injections. The injections were performed at a depth of 120 μm , with a volume of 40 μl in 3 injections (2 right flank, 1 left flank) and with a rate of 10 $\mu\text{l}/\text{min}$. The depth was increased up to 200 μm if leakage was observed at the beginning of injection. In all experiments a total of 5 μg OVA or 50 μg OVA peptides were injected per immunization. In case of anPLGA-OVA-PIC, the dose of poly(I:C) was also 5 μg . Ethical approval was given by the Animal Ethics Committee from Utrecht University, The Netherlands.

2.6. Adoptive transfer of OVA T cell receptor (TCR) tg T cells

OVA-specific T cell transferred mice were obtained by injecting OT-I CD8⁺ and OT-II CD4⁺ T cells into wildtype B6-SJL mice. In order to obtain OT-I and OT-II cells, spleens were isolated from OT-I and OT-II mice and erythrocyte-depleted splenocytes were obtained as follows. Single cell suspensions were prepared by passage over a 70 μm cell strainer after homogenizing the spleens with a syringe plunger, in RPMI 1640 GlutaMAX supplemented with 8.5% fetal calf serum (Bodinco), 30 μM 2-mercaptoethanol and penicillin/streptomycin (complete RPMI medium). The erythrocytes were depleted by lysis with ACK lysis buffer. Transgenic naïve CD4⁺ (OT-II) cells and transgenic CD8⁺ (OT-I) cells were isolated from splenocytes by negative selection using Magnetic DynaBeads® (Thermo Fisher Scientific, Waltham, MA). Antibodies used were $\alpha\text{CD}11\text{b}$, $\alpha\text{MHC-II}$, $\alpha\text{B}220$ and either $\alpha\text{CD}4$ for CD8 (OT-I) T cell purification or $\alpha\text{CD}8$ and $\alpha\text{CD}25$ for naïve CD4⁺ (OT-II) T cell purification. After negative selection by magnetic beads, a purity around 70% was achieved for naïve tg CD4⁺ (OT-II) T cells. An additional sorting was necessary to separate naïve from non-naïve tg CD8⁺ (OT-I) T cells. After selection on CD8⁺, CD44^{low} and CD62L^{high} using a BD influx, 100% purity of naïve tg CD8⁺ (OT-I) T cells was obtained. Naïve tg CD4⁺ (OT-II) T cells were stained with carboxy-fluorescein succinimidyl ester (CFSE; 0.5 μM , Invitrogen) and naïve tg CD8⁺ (OT-I) T cells were stained with Cell trace violet (CTV; 5 μM , Invitrogen) for 10 min at 37 °C. A total of 2×10^6 CFSE-labelled naïve tg CD4⁺ T cells and 1×10^6 CTV-labelled naïve tg CD8⁺ cells were injected into the tail vein of recipient mice, one day before immunization to obtain OVA-specific T cell transferred mice.

2.7. In vivo proliferation of adoptively transferred T cells

OVA-specific T cell transferred mice were immunized with OVA, anPLGA-OVA and catPLGA-OVA at day 0. PBS and OVA peptide immunizations were used as negative and positive controls, respectively. Proliferation of tg T cells was studied at day 3, 5 and 7. Next, 2.5×10^6 erythrocyte depleted splenocytes or draining (inguinal) lymph node cells were stained with $\alpha\text{CD}45.2$, $\alpha\text{CD}4$ and $\alpha\text{CD}8$ and transferred cells were measured as a percentage of CD45.2⁺ and either CD8⁺ or CD4⁺ cells of total cells using a FACSCanto II (BD Biosciences) and FlowJo (TriStar) analysis software. Percentages of fully proliferated (> 6 division) transferred cells were measured by similar antibody staining, but as CD45.2⁺ and either CTV⁻ CD4⁺ and CFSE^{low} or as CFSE⁻ CD8⁺ and CTV^{low}, all after gating on live cells on FSC-A/SSC-A and single cells in

FSC-A/FSC-H.

2.8. Endogenous CD4⁺ and CD8⁺ T cell response

B6-SJL mice were immunized with OVA, OVA + poly(I:C), anPLGA-OVA, catPLGA-OVA or anPLGA-OVA-PIC at day 0, 3, 6 and T cell responses were analyzed at day 13. The endogenous CD4⁺ T cell response was measured by ³H thymidine incorporation. For this 0.2×10^6 erythrocyte-depleted splenocytes or inguinal lymph node cells were plated in complete RPMI medium in a 96 well round bottom plate for 72 h with or without 10 $\mu\text{g}/\text{ml}$ OVA Endo-Fit (Worthigton) or ConA, at 37 °C in a humidified incubator. After 72 h, ³H-Thymidine (0.4 $\mu\text{Ci}/\text{well}$; Amersham Biosciences Europe GmbH) was added for an additional 18 h and incorporation into DNA was measured by liquid scintillation counting (Microbeta, Perkin-Elmer Inc.).

CD8⁺ T cell activation was measured using intracellular IFN γ staining as described previously [26]. In short, 2.5×10^6 erythrocyte-depleted splenocytes were incubated in complete RPMI medium with 1 $\mu\text{g}/\text{ml}$ pOVA_{257–264} (Genscript) or complete RPMI medium and 10 μM monensin (eBioscience) for 6 h at 37 °C in 6% humidified incubator. Cells were stained with either $\alpha\text{CD}8$ antibody, $\alpha\text{CD}4$, $\alpha\text{CD}62\text{L}$ or $\alpha\text{CD}44$ in the presence of $\alpha\text{CD}16/\text{CD}32$ to block Fc-receptors. Next, they were fixed with 2% paraformaldehyde and stained with $\alpha\text{IFN}\gamma$ antibody in the presence of 0.05% saponin. Samples were measured on a FACSCanto II (BD Biosciences) and analyzed using FlowJo software (Tree Star).

2.9. CFU counts in bacterial challenge study

B6-SJL mice were immunized with OVA, OVA + PIC, anPLGA-OVA, catPLGA-OVA or anPLGA-OVA-PIC at day 0, 3 and 6. Mice were challenged with recombinant *Listeria monocytogenes* secreting OVA (rLM-OVA) 21 days after final immunization. Mice immunized with 10.000 CFU rLM-OVA at day 6 were used as positive control and unimmunized mice served as negative control. rLM-OVA [27,28] were cultured in Brain Hart Infusion broth (BHI; Sigma-Aldrich) with 5 $\mu\text{g}/\text{ml}$ erythromycin and to challenge the mice 100.000 bacteria from a LOG-phase culture were injected in 200 $\mu\text{l}/\text{mouse}$ in the tail vein. To study the elimination of bacteria, three days after challenge spleens were isolated and single cell suspensions were made in RPMI medium. Serial dilutions were plated on BHI agar plates and CFU counts were determined after approximately 36 h in a 37 °C incubator. The remaining mice were sacrificed 5 days after the challenge to study the CD4⁺ and CD8⁺ T cell response. The specific T cell response was determined in spleen using intracellular IFN- γ staining method as described in section 8. To determine the memory phenotype of the CD8⁺ T cells, CD62L and CD44 antibodies were used. First, in the gate of the total CD8⁺ T cells, three different populations were gated (Supplementary Fig. 1B; solid lines). CD44⁻ were considered naïve T cells, CD44⁺CD62L⁺ are T central memory cells and CD44⁺CD62L⁻ are T effector and T effector memory cells. Second, in order to determine the antigen specific memory phenotype, the gates that were set on all CD8⁺ T cells were copied in the CD8⁺IFN γ ⁺ population.

2.10. Statistics

Statistical significance was determined using Kruskal-Wallis and multiple comparison/post hoc analysis was done with Dunn's correction, * = $p < 0.05$, ** = $p < 0.01$, *** = $p < 0.001$.

3. Results

3.1. Preparation and characterization of PLGA nanoparticles

The physicochemical characteristics of PLGA nanoparticles are shown in Table 1. PLGA nanoparticles had a size of approximately

Table 1
Physicochemical characteristics of PLGA nanoparticles.

| Nanoparticles | Size (nm) | PDI | ZP (mV) | EE% | | LC% | |
|----------------|-------------|---------------|-------------|-------------|-----------|------------|-----------|
| | | | | OVA | Poly(I:C) | OVA | Poly(I:C) |
| anPLGA-OVA | 155.0 ± 6.2 | 0.064 ± 0.010 | -18.2 ± 1.7 | 54.8 ± 1.0 | - | 6.6 ± 0.1 | - |
| catPLGA-OVA | 147.3 ± 2.1 | 0.100 ± 0.029 | 9.9 ± 0.5 | 87.0 ± 4.8 | - | 10.4 ± 0.6 | - |
| anPLGA-OVA-PIC | 148.4 ± 8.4 | 0.032 ± 0.007 | -17.4 ± 0.8 | 47.2 ± 16.2 | 9.6 ± 2.8 | 2.8 ± 1.0 | 2.7 ± 0.8 |

150 nm with a low PDI ranging from 0.032 to 0.100. AnPLGA-OVA had a negative surface charge with a zeta potential of approximately -18 mV and catPLGA-OVA possessed a positive surface charge with an opposite zeta potential around +10 mV. The EE% of OVA was approximately 50% in both anPLGA-OVA and anPLGA-OVA-PIC, and catPLGA-OVA showed a significantly higher EE%. CatPLGA-OVA had also a higher LC% (10.4%) of OVA than anPLGA-OVA (6.6%) and anPLGA-OVA-PIC (2.8%). The ratio between the initial amounts of OVA and poly(I:C) in the formulations during the preparation procedure was adjusted in order to prepare anPLGA-OVA-PIC with similar LC% of OVA (2.8%) and poly(I:C) (2.7%).

The formulations are characterized in terms of size (diameter) and poly disperse index (PDI), zeta potential (ZP), and encapsulation efficiency (EE) and loading capacity (LC) of OVA and poly(I:C). The EE% of OVA or poly(I:C) was defined as the percentage of encapsulated amount of OVA or poly(I:C) compared to the added amount of OVA or poly(I:C). The LC% of OVA or poly(I:C) was defined as the percentage of encapsulated amount of OVA or poly(I:C) compared to the amount of nanoparticles. anPLGA-OVA: OVA-loaded PLGA nanoparticles with negative surface charge. catPLGA-OVA: OVA-loaded PLGA nanoparticles with positive surface charge. anPLGA-OVA-PIC: OVA and poly(I:C) co-encapsulated anionic PLGA nanoparticles.

3.2. Release of OVA and poly(I:C) from PLGA nanoparticles

Release of OVA and poly(I:C) from PLGA nanoparticles was measured *in vitro* in culture medium containing serum (Fig. 1). The developed nanoparticles showed a burst release of OVA within the first day, followed by a slow release. At day 30 approximately 49%, 22% and 26% OVA was released from anPLGA-OVA, catPLGA-OVA and anPLGA-OVA-PIC, respectively. In case of poly(I:C), anPLGA-OVA-PIC followed the trend of OVA. At day 30, around 42% poly(I:C) was released. Thus, all of the PLGA nanoparticles released at most one half of their content within one month time.

3.3. OVA-loaded PLGA nanoparticles enhances antigen-induced activation of tg T helper cells and enables priming of tg cytotoxic T cells after intradermal immunization using a hollow microneedle

To determine the induction of a cellular immune response towards a protein antigen that is delivered via hollow microneedles, we first examined the ability of a protein antigen to activate transgenic (tg) T cells that were adoptively transferred (Fig. 2A). Naïve OVA specific CD4⁺ and CD8⁺ T cells were isolated from spleens of OT-II and OT-I mice, expressing a tg T Cell Receptor specific for the CD4⁺ and CD8⁺ T cell epitopes (OVA_{323–339} and OVA_{257–264}) of the model antigen OVA, respectively [29,30]. After staining with cell trace dyes, these cells were mixed and transferred into congenic recipient mice, allowing the distinction between host and donor T cells in flow cytometry, based on expression of the congenic marker (Fig. 2A). One day later the recipient mice were immunized intradermally, using a hollow microneedle, with full length OVA protein or with the OVA epitopes (pOVA). These epitopes do not require any antigen processing in order to activate tg T cells and served as a positive control. We first determined if CD4⁺ T helper cells were activated in the present study. Tg CD4⁺ T cells were detected in flow cytometry as CD4⁺ CD45.2⁺ T cells within the

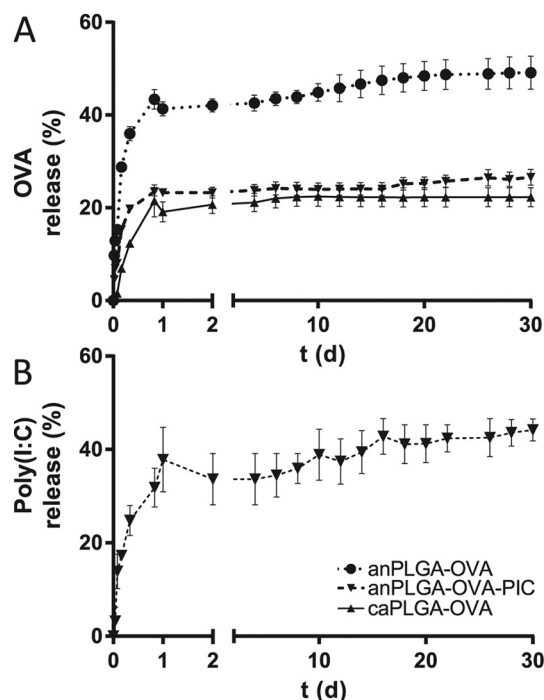


Fig. 1. Release of OVA and poly(I:C) from PLGA nanoparticles. PLGA nanoparticles were dispersed into culture medium containing serum and incubated at 37 °C. At different time points, the release sample was collected to determine the release amount of OVA (A) and poly(I:C) (B). Data is presented as mean ± SEM, n = 3.

lymphocyte gate in either draining inguinal lymph nodes (dLN) or in the spleens. In OVA protein-immunized mice, a small increase in numbers of tg CD4⁺ T cells compared to PBS group was found in the dLN at day 5 after immunization, while in mice immunized with peptides numbers of tg CD4⁺ T cells were higher in both dLN and spleen (Fig. 2B). In mice immunized with OVA protein, minimal systemic responses were measured in the spleen at day 7 (Fig. 2C, F), and furthermore, minimal numbers of transferred CD4⁺ T cells activated by OVA protein were fully proliferated (Fig. 2D-F; depicted by > 6 dilutions of cell trace dye).

We then determined whether OVA encapsulation in PLGA nanoparticles could enhance OVA-specific tg CD4⁺ T cell responses. When mice were immunized with OVA-loaded anionic and cationic PLGA nanoparticles (PLGA-OVA), we detected high numbers of OVA-specific tg CD4⁺ T cells in dLN, both at day 5 and 7 post-immunization (Fig. 2B). And in spleen these numbers were also significantly higher (Fig. 2C) than in mice immunized with soluble OVA. Total numbers of tg CD4⁺ T cells retrieved from PLGA nanoparticle immunized mice were also much higher than in mice immunized with peptide (Fig. 2B, C). Over 95% of these cells were fully proliferated in anPLGA-OVA and catPLGA-OVA groups, while OVA induced only slightly more fully proliferated cells than PBS locally on day 5 and systemically on day 7. Immunizing with the OVA peptides showed a high proliferation rate at day 5 only, while at day 7 the numbers of fully proliferated cells dropped (Fig. 2E-F). No differences were observed between responses

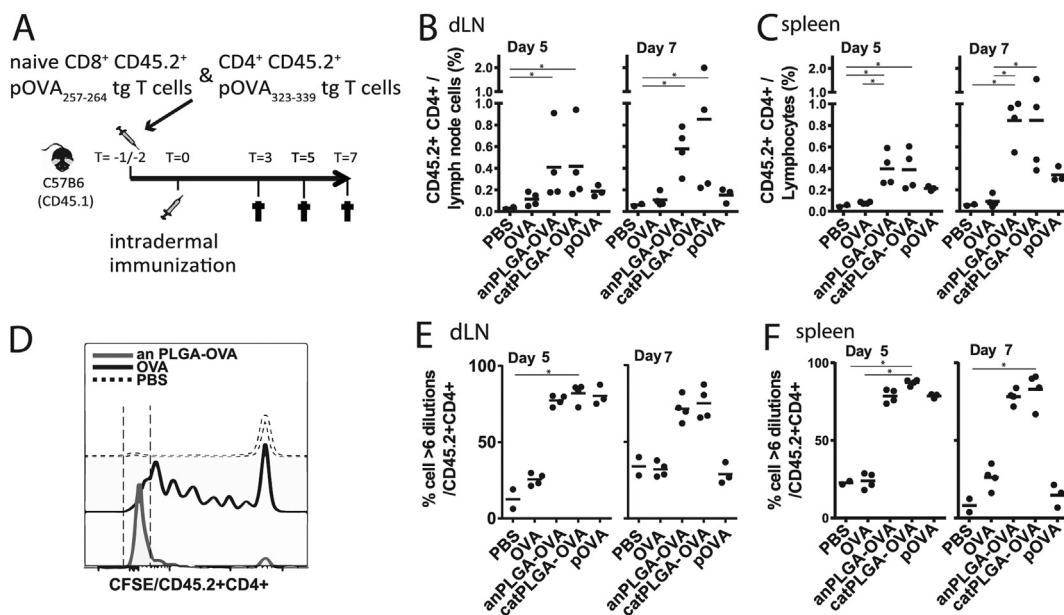


Fig. 2. Encapsulation of OVA by PLGA nanoparticles enhances activation of tg $CD4^+$ T cells after intradermal immunization using hollow microneedle.

(A) Experimental design; naive $CD8^+$ tg T cells specific for $OVA_{257-264}$ were isolated from spleens of OT-I mice and stained with Cell Trace Violet. $CD4^+$ tg T cells specific for $OVA_{323-339}$ were isolated from spleens of OT-II mice and stained with carboxyfluorescein succinimidyl ester (CFSE). From both cell types 1×10^6 cells were injected in tail vein of B6-SJL mice 1 or 2 days before intradermal immunization. T cell responses were analyzed on day 3, 5 and 7. (B–F) $CD4^+$ T cell response of tg transferred T cells. (B–C) Amount of transferred tg T cells as percentage of $CD45.2^+ CD4^+$ cells in either dLN cells or lymphocyte gate of splenocytes. (D) Indication of fully proliferated (> 6 dilutions) cells in the CFSE window of $CTV^- / CD45.2^+ CD4^+$ / lymphocyte gate. (E–F) Percentage of cells that are $CD45.2^+ CD4^+$ and divided > 6 times as measured by CFSE intensity on day 5 or 7 in either dLN (E) or spleen (F) after intradermal immunization via hollow microneedles with the formulations indicated on x axes. Graphs are representative for 1 of total 2 independent experiments. Per experiment the number of mice used is $n = 4$ for OVA, anPLGA-OVA and catPLGA-OVA immunization groups, $n = 3$ for pOVA immunization groups, $n = 2$ for PBS immunization group (as depicted by the number of symbols in the graph). Statistical significance was determined using Kruskal-Wallis, $p < 0.05$ and multiple comparison/post hoc analysis was done comparing immunization strategies versus PBS or OVA immunization with Dunn's correction, $^*p < 0.05$.

detected against anPLGA-OVA and catPLGA-OVA. Taken together, we show that encapsulation in PLGA nanoparticles enhanced the activation of tg T helper cells by OVA after intradermal immunization using hollow microneedles.

Next, it was determined if the followed immunization strategy also induced a cytotoxic cellular immune response, to provide protection against intracellular pathogens or tumors. Activation and proliferation of $CD8^+$ tg T cells was measured in the same experimental setup as shown in Fig. 2A. As expected, no increase in the numbers of tg $CD8^+$ T cells was detected in either dLN or spleen at day 3, 5 or 7 after immunization with soluble OVA protein (Fig. 3A, B). On day 3, immunization with OVA induced some T cell proliferation, as shown by dilution of cell trace dye (Fig. 3C, D), although this proliferation did not lead to a significant increase in tg $CD8^+$ T cell numbers (Fig. 3A, B). In contrast, immunization with OVA-loaded PLGA nanoparticles, induced a marked increase in tg $CD8^+$ T cell numbers not only in dLN but also in spleen, as detected at both days 5 and 7 (Fig. 3A, B). Most of these cells were fully proliferated and there was no difference observed between responses induced by anPLGA-OVA and catPLGA-OVA. Immunization with OVA peptides also induced a systemic tg $CD8^+$ T cell response, detected at day 5, but in contrast to nanoparticle-immunization, this response decreased significantly at day 7 in spleen as well as dLN. This was probably due to differing kinetics of T cell responses triggered by precise T cell epitopes, compared to full length OVA, which requires prior antigen processing. In conclusion, our data indicate that encapsulation in PLGA nanoparticles enables OVA to trigger $CD8^+$ tg T cell responses upon hollow microneedle-mediated intradermal delivery.

3.4. OVA primes both endogenous $CD4^+$ and $CD8^+$ T cell responses in immunized hosts when particulated in PLGA nanoparticles or adjuvanted with TLR3 agonist

Having shown that hollow microneedle-mediated immunization

with OVA-loaded PLGA nanoparticles activates adoptively transferred tg T cells (Figs. 2 and 3), we next examined whether this strategy also primes endogenous T cell responses in immunized hosts. To this end, wild type mice were immunized at day 0, 3 and 6 with either OVA, OVA adjuvanted with TLR3 agonist poly(I:C) (OVA + PIC), anPLGA-OVA, catPLGA-OVA or anPLGA-OVA-PIC (Table 1; Fig. 4A).

At day 13, antigen-specific $CD8^+$ T cell responses were detected by intracellular $IFN\gamma$ cytokine staining (Supplementary Fig. 1A). Background levels of $IFN\gamma$ produced by $CD8^+$ T cells was low in all mice, as depicted by restimulation of cells with medium (Fig. 4B, C). As expected, no $OVA_{257-264}$ -specific $CD8^+$ T cell response was detected in mice immunized with soluble OVA (Fig. 4B, C). In contrast, responses to this epitope were clearly detectable in dLN (Fig. 4B) and the spleen (Fig. 4C) of mice immunized with either OVA + PIC, as well as catPLGA-OVA or anPLGA-OVA. Responses in the anPLGA-OVA mouse group tended to be lower than in the catPLGA-OVA group. The addition of poly(I:C) enhanced the response induced by anPLGA-OVA immunization, although OVA-PIC only already showed some $CD8$ activation as well (Fig. 4B, C). Thus, following hollow microneedle-mediated delivery, a specific recipient $CD8^+$ T cell response is induced by OVA when encapsulated in cationic PLGA nanoparticles or when adjuvanted with TLR3 agonist with or without anionic PLGA nanoparticles.

Furthermore, induction of OVA-specific $CD4^+$ T cell responses in the immunized mice was determined by measuring 3H -thymidine incorporation in 72 h splenocyte cultures incubated with OVA protein. Some OVA-specific proliferation was detected in mice immunized with OVA + PIC, catPLGA-OVA, and anPLGA-OVA-PIC (Fig. 4D), although no significant differences between groups were observed.

Thus, hollow microneedle-mediated, intradermal immunization with PLGA nanoparticle encapsulated OVA with or without poly(I:C) induces clearly detectable $OVA_{257-264}$ -specific $CD8^+$ T cell responses and minor OVA-specific $CD4^+$ T cell responses in mice.

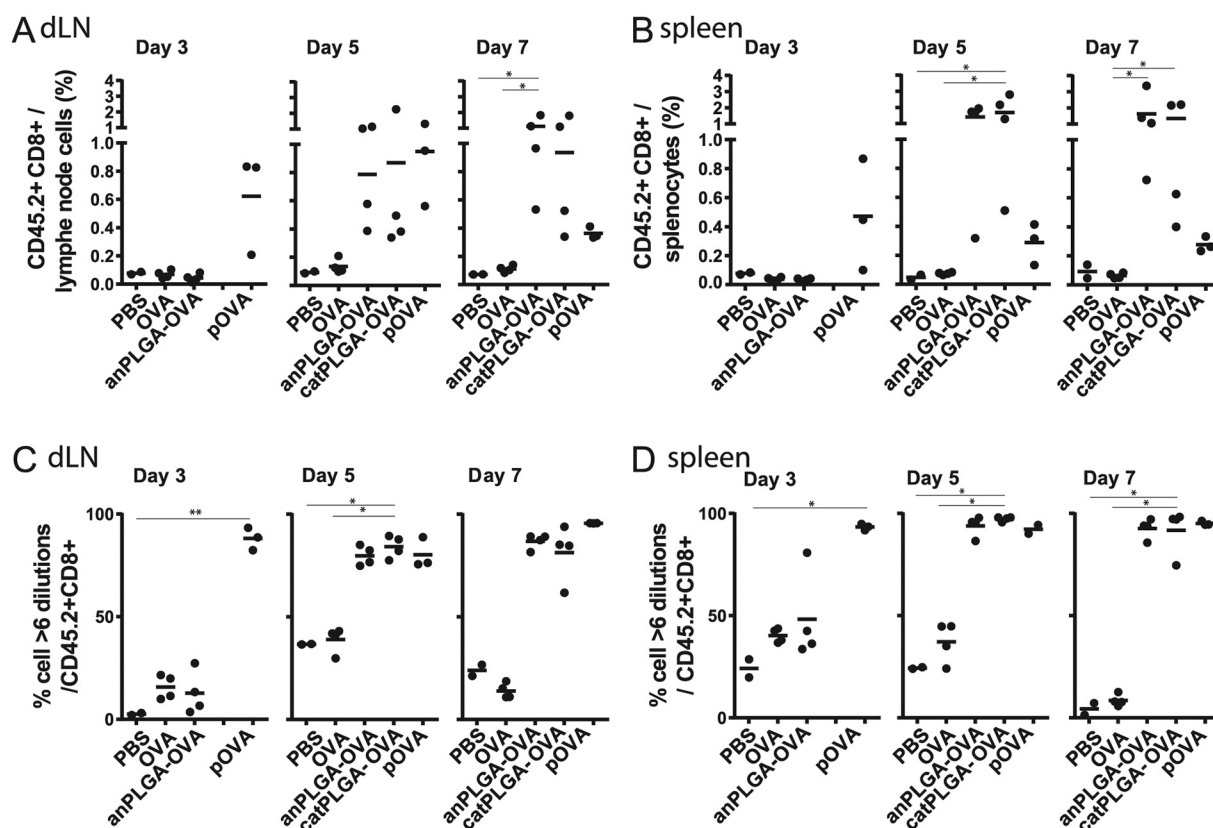


Fig. 3. Encapsulation of OVA by PLGA nanoparticles enables activation of tg CD8⁺ T cells after intradermal immunization using hollow microneedle. CD8⁺ T cell response of tg transferred T cells. (A, B) Amount of transferred tg T cells as percentage of CD45.2⁺ CD8⁺ cells in either dLN cells or lymphocyte gate of splenocytes. (C, D) Percentage of cells that are CD45.2⁺ CD8⁺ and divided > 6 times as measured by Cell Trace Violet intensity on day 3, 5 or 7 in either dLN (C) or spleen (D) after intradermal immunization via hollow microneedles with the formulations indicated on X-axes. Graphs are representative for 1 of total 2 independent experiments. Per experiment the number of mice used is $n = 4$ for OVA, anPLGA-OVA and catPLGA-OVA immunization groups, $n = 3$ for pOVA immunization groups, $n = 2$ for PBS immunization group (as depicted by the number of symbols in the graph). Statistical significance was determined using Kruskal-Wallis, $p < 0.05$ and multiple comparison/post hoc analysis was done comparing immunization strategies versus PBS immunization with Dunn's correction, $*p < 0.05$.

3.5. Protective immune response towards recombinant rLM-OVA after intradermal immunization using hollow microneedles

CD8⁺ T cells play an essential role in clearance of the intracellular bacterium *Listeria monocytogenes* [31]. Next, we determined whether hollow microneedle-mediated vaccination with PLGA nanoparticles induces protective immunity against rLM-OVA. Mice were immunized with OVA, OVA-PIC, anPLGA-OVA, catPLGA-OVA or anPLGA-OVA-PIC at day 0, 3 and 6 and challenged with the bacterium, 21 days after final immunizations (Fig. 5A). Unimmunized mice served as a negative control and mice immunized with rLM-OVA at day 6 served as positive control, as these mice are typically able to completely clear the bacterium within 3 days after challenge. Determination of CFU counts in the spleens at day 30 showed that mice immunized with rLM-OVA indeed completely cleared the challenge dose, while spleens of non-immunized mice contained on average approximately 100,000 bacteria (Fig. 5B). While immunization with soluble OVA, anPLGA-OVA or OVA-PIC failed to protect (Fig. 5B), protection was observed in at least one mouse immunized with catPLGA-OVA. Moreover, anPLGA-OVA-PIC induced full protection, resulting in zero bacteria count in the spleen, similar to mice immunized with rLM-OVA. This indicates that immunization with anPLGA-OVA-PIC, and to some degree catPLGA-OVA, via the intradermal route using hollow microneedles, elicits a protective cellular immune response.

To study the possible relation between T cell response and the capacity to clear the pathogen, the T cell response in the spleen of the mice was measured. Quantification of T cell responses 5 days after challenge with rLM-OVA showed that all immunization regimens

triggered OVA-specific CD4⁺ T cell responses, and that poly(I:C) did not further increase these responses (Fig. 5C). In all immunized groups except for OVA-immunized mice a particularly robust activation of antigen-specific CD8⁺ T cells was detected (Fig. 5D). Remarkably, the minor population of activated CD8⁺ T cells in OVA-immunized mice consisted of 40% central memory T cells (Tcm; CD62L⁺ CD44⁺) and 60% effector T cells and effector memory T cells (Teff/Tem; CD62L⁻ CD44⁺). In contrast, in the other immunization groups the Tcm populations were much smaller and the Teff/Tem cell population much larger (Supplementary Fig. 1B–D; solid line). While Tcm:Teff/Tem cell ratio failed to correlate with immune protection, cells within the CD62L⁻ CD44⁺ gate were further analyzed (Supplementary Fig. 1B–D; dotted line). We found higher CD44^{int}:CD44^{hi} cell ratios in mice that had received anPLGA-OVA-PIC, catPLGA-OVA and rLM-OVA, i.e. the immunization regimens that led to reduced CFU counts following bacterial challenge (Fig. 5E). Thus, the presence of antigen-specific CD44^{int} CD8⁺ T cells seems favorable for immune protection to rLM-OVA infection.

4. Discussion

Nowadays, most of the vaccines under investigation are based on recombinant proteins or subunits of pathogens, because of improved safety and lower production cost compared to live or attenuated vaccines [32]. However, generally such vaccines are poorly immunogenic and fail to elicit robust cell-mediated immunity against intracellular pathogens. In this respect, nanoparticle-based delivery of antigens may be an attractive tool, because it can improve immune response

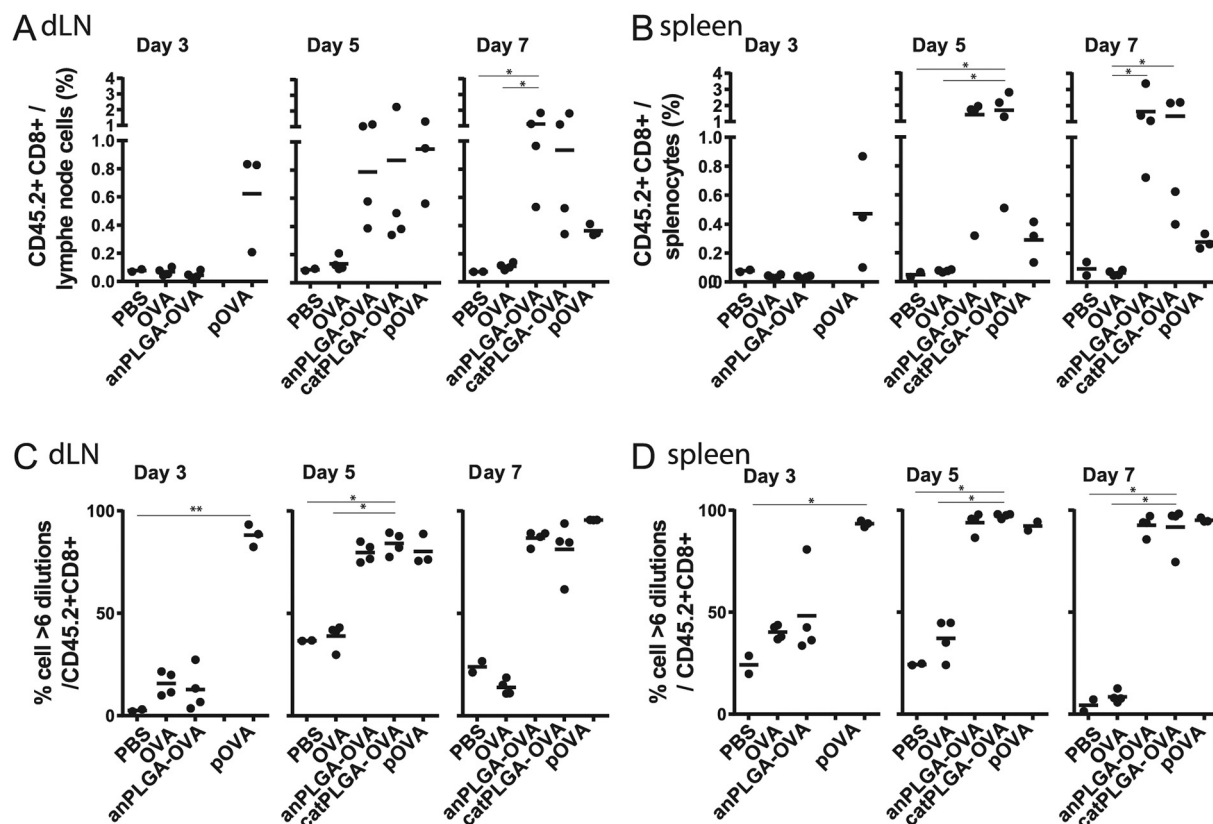


Fig. 4. Specific endogenous T cell responses induced by OVA when particulated in anionic or cationic PLGA nanoparticles or when adjuvanted with TLR3 agonist.

(A) Schematic overview of immunization strategy of measuring wild type T cell responses. Intradermal immunization on day 0, 3 and 6 and responses measured 7 days after final immunization (day 13). (B, C) Percentage of IFN γ ⁺ cells in CD8⁺ gate within the lymphocyte gate on FSC/SSC of dLN (B) or spleens (C) depicted in black symbols. IFN γ ⁺ cells upon stimulation with medium is considered background and shown in gray. Results were pooled of 2 experiments with a total of 6–9 mice/group. (D) CD4⁺ T cell response was measured by proliferation of splenocytes upon stimulation of OVA protein. Incorporation of ³H-thymidine in DNA was measured liquid scintillation counting as CCTM. Statistical significance was determined using Kruskal-Wallis, $p < 0.05$ and multiple comparison/post hoc analysis was done comparing all immunization groups with Dunn's correction, * $p < 0.05$, ** $p < 0.01$, *** $p < 0.001$.

induction to encapsulated antigens [33]. In this study, OVA was used as a model antigen and encapsulated into PLGA nanoparticles with or without the adjuvant poly(I:C). The capacity of the nanoparticle formulations to stimulate cell-mediated immunity was investigated by intradermal immunization using hollow microneedles. In this study, we show that intradermal delivery using hollow microneedles can elicit a protective cellular immune response when the antigen is encapsulated in cationic or adjuvanted anionic PLGA nanoparticles. These data expand on previous studies using hollow microneedles where humoral immune responses were detected [7–9], which illustrated the attractiveness of the intradermal route for the delivery of vaccines. In our studies, we elaborated on the potential to induce CD8⁺ T cells in the skin using microneedles, specifically using hollow microneedles.

Nanocarriers used for delivery of proteins or subunit vaccines enhance antigen uptake by antigen presenting cells and contribute to a prolonged presentation of the vaccine antigen at the cell surface [34,35]. This leads to activation of a cellular immune response, which was exemplified in previous studies showing that PLGA nanoparticle-encapsulated antigens, with or without adjuvant, may induce strong T helper type 1 and cytotoxic T cell immune response (Th1/CTL) response when delivered systemically or subcutaneously [15,17,36]. However, relatively little is known about the immune responses elicited by nanoparticle vaccines when administered intradermally using microneedles. On the one hand, inducing conduits in the skin with microneedles and subsequent application of nanoparticles, loaded with either OVA or antigen-encoding cDNA, induced an immune response [37,38]. Nevertheless, this method of delivery differs from intradermal administration by microneedles. On the other hand, some previous studies on

model subunit vaccines using microneedles, such as nanopatches to deliver non-encapsulated TLR adjuvants or pH sensitive microneedles arrays loaded with high doses of protein induced CD8⁺ T cell responses [39–41]. However, in these studies using microneedles none of the vaccine antigens were encapsulated in nanoparticles. In one study, dissolving microneedles loaded with PLGA nanoparticle encapsulated antigens were used for intradermal vaccination, and shown to induce a robust antigen-specific protective cellular immune response in mice [24].

Our data show that hollow microneedle-delivered nanoencapsulated OVA not only activated transferred tg T cells, but also primed endogenous protective CD8⁺ T cell responses in immunized mice. In mice adoptively transferred with tg T cells, an endogenous T cell response could not be detected (not shown). This may be explained by the single injection immunization regimen in these studies, which may be sufficient to prime adoptively transferred tg CD8⁺ T cells, but not the naïve antigen-specific T cell repertoire. Alternatively, interference of the relatively easily activated tg T cells with priming of naïve T cells of recipient mice, for example by cytotoxicity towards antigen presenting pAPC as part of an immune homeostasis feedback loop, may also explain this observation. For this reason, to examine whether hollow microneedle-mediated immunization with PLGA nanoparticles encapsulated OVA may prime OVA-specific endogenous CD8⁺ T cells in mice, a priming procedure was used consisting of three immunizations delivered over a time period of 6 days. This protocol had been shown to induce cellular immune responses following dermal DNA tattoo immunization [26,42], but not yet when using hollow microneedles [7]. We report here that this prime boost protocol indeed elicits vigorous

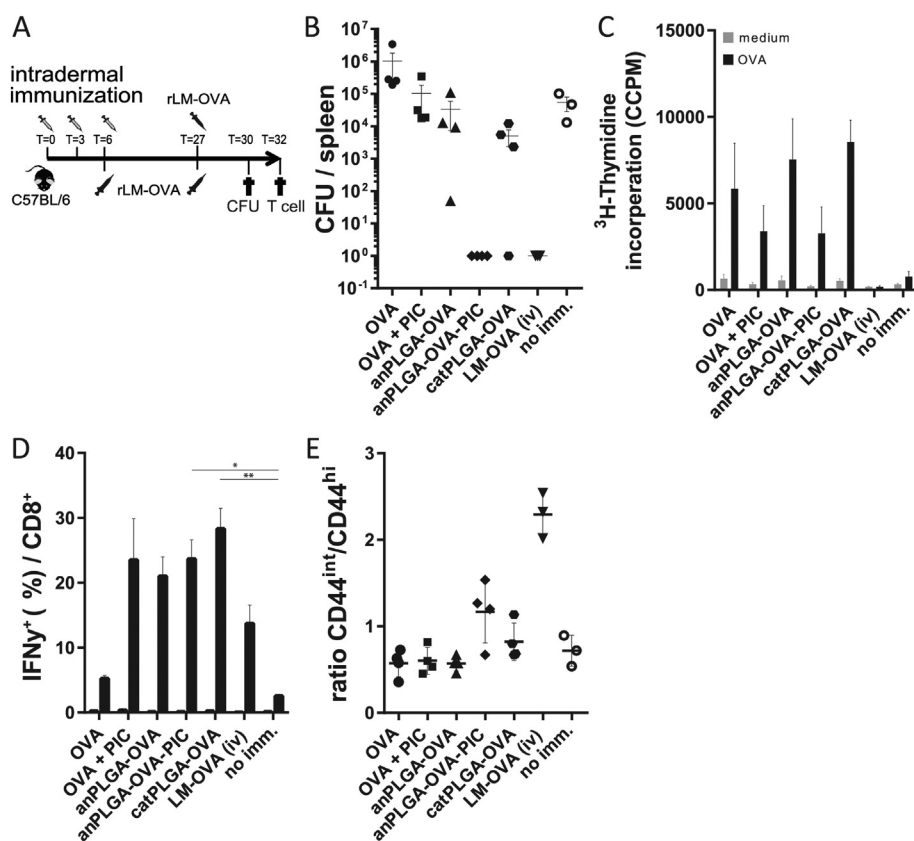


Fig. 5. Protective immune response towards rLM-OVA after hollow microneedle mediated intradermal immunization (A) Schematic overview of challenge study in which the mice received an i.v. challenge of 100,000 recombinant *Listeria monocytogenes*-OVA 21 days after 3 immunizations with OVA with or without negatively or positively charged PLGA NP or with or without poly(I:C). CFU count of rLM-OVA in spleen was determined 3 days after challenge and T cell activation was measured 5 days after challenge. (B) Spleens were isolated and serial dilutions were plated on BHI agar plates and CFU's were counted 36 h after incubation at 37 °C. (C) CD4⁺ T cell and (D + E) CD8⁺ T cell responses were measured identical to procedure Fig. 3B + D in spleens. Gentamycin was added to culture medium to prevent further growth of potential rLM-OVA. Per experiment $n = 4$ for OVA, anPLGA-OVA and catPLGA immunization groups, $n = 3$ for pOVA immunization groups, $n = 2$ for PBS immunization group (as depicted by the number of symbols in the graph). Statistical significance was determined using Kruskal-Wallis, $p < 0.05$ and multiple comparison/post hoc analysis was done with Dunn's correction, * $p < 0.05$.

CD8⁺ T cell responses in mice immunized with PLGA encapsulated antigen, when using hollow microneedles as delivery method.

A variety of dendritic cells in the dermis and epidermis have been shown to contribute to immune activation following dermal immunization [43,44], and they all express diverse pathogen recognition receptors, such as Toll-like receptors (TLRs). In agreement with this observation, multiple intradermal immunization studies using different administration methods have shown added effects of different Toll-like receptor (TLR) agonists based adjuvants [16,45]. In our study, co-delivery of OVA and the TLR3 agonist poly(I:C) in PLGA nanoparticles, led to protective cellular immune responses to rLM-OVA. Possibly, the nanoparticles act as a depot system and stimulate the immune system by controlling the release of OVA and poly(I:C), resulting in prolonged OVA presentation and enhanced immunogenicity [23].

Positively charged cationic PLGA nanoparticles are considered to be more immunogenic than anionic PLGA nanoparticle, as their positive surface charge facilitate the interaction with anionic cell membranes, enhancing uptake of these nanoparticles by phagocytic cells [46]. However, this enhanced interaction can also lead to increased cell cytotoxicity [10], contributing to the challenges faced for therapeutic use in humans. In our adoptive transfer studies anPLGA-OVA and catPLGA-OVA seemed to perform equally well. However, catPLGA-OVA primed the endogenous cellular immune responses efficiently, while anPLGA-OVA did not show significant increase of response compared to OVA. Although one mouse showed full protection from subsequent infection with rLM-OVA after immunization with catPLGA-OVA, no statistical difference in degree of immune protection induced by cationic compared to anionic PLGA-OVA was detected. Inclusion of poly(I:C) in the anionic nanoparticles was needed to fully protect immunized mice from infection.

Remarkably, although immune protection differed between mice immunized with OVA particulated in cationic or anionic PLGA without or with poly(I:C), vigorous OVA-specific CD8⁺ T cell responses were detected in all mouse groups except for mice immunized with soluble

OVA. Difference in antigen release can have a role in shaping the memory phenotype [47], however we found similar release profiles. Further analysis of CD8⁺ T cell phenotype showed that there was no difference within percentage of T_{cm} and T_{em}/T_{eff} cells between the different PLGA NP immunized groups, but an enhanced ratio of CD8⁺ T cells with CD44^{int} phenotype was detected in mice immune to rLM-OVA challenge. Thus, although no clear definition of CD44^{int}CD62L^{neg} is available [48–50], we show a correlation between their presence and intradermal immunization-induced protective immunity to challenge with rLM-OVA.

Taken together, we show that hollow microneedles are an excellent tool for intradermal vaccination, leading to the induction of minor CD4⁺ T cell and vigorous CD8⁺ T cell responses to PLGA nanoparticle encapsulated antigens. Evoked CD8⁺ T cell responses provided protection against an intracellular bacterium if poly(I:C) was co-encapsulated with the OVA antigen. Future studies may show whether other adjuvants have similar effects or whether specific adjuvants may induce protection to specific categories of intracellular pathogens.

Supplementary data to this article can be found online at <http://dx.doi.org/10.1016/j.jconrel.2017.09.017>.

Acknowledgements

The research leading to these results has received support from the Innovative Medicines Initiative Joint Undertaking under grant agreement no. [115363], resources of which are composed of financial contribution from the European Union's Seventh Framework Programme (FP7/2007-2013) and EFPIA companies' in kind contribution. Furthermore, G. Du acknowledges for part support from Chinese Council Scholarship. Furthermore, we wish to thank I.S. Ludwig, P.J.S. van Kooten, and M.A.A. Jansen, Utrecht University, Utrecht, The Netherlands, for technical assistance. Graphical abstract has been made by adapting images from the Servier medical art bank by Servier on servier.com.

References

- [1] C. Levin, H. Perrin, B. Combadiere, Tailored immunity by skin antigen-presenting cells, *Hum. Vaccin Immunother.* 11 (1) (2015) 27–36.
- [2] K. van der Maaden, W. Jiskoot, J. Bouwstra, Microneedle technologies for (trans) dermal drug and vaccine delivery, *J. Control. Release* 161 (2) (2012) 645–655.
- [3] Y. Kim, J. Park, M. Prausnitz, Microneedles for drug and vaccine delivery, *Adv. Drug Deliv. Rev.* 64 (14) (2012) 1547–1568.
- [4] E. Larraneta, M.T.C. McCrudden, A. Courtenay, R. Donnelly, E. Larrañeta, Microneedles: a new frontier in nanomedicine delivery, *Pharm. Res.* 33 (5) (2016) 1055–1073.
- [5] M. Prausnitz, Microneedles for transdermal drug delivery, *Adv. Drug Deliv. Rev.* 56 (5) (2004) 581–587.
- [6] H. Quinn, M. Kearney, A. Courtenay, M.T.C. McCrudden, R. Donnelly, The role of microneedles for drug and vaccine delivery, *Expert Opin. Drug Deliv.* 11 (11) (2014) 1769–1780.
- [7] K. Van Der Maaden, S.J. Trietsch, H. Kraan, E.M. Varypataki, S. Romeijn, R. Zwier, et al., Novel hollow microneedle technology for depth-controlled microinjection-mediated dermal vaccination: a study with polio vaccine in rats, *Pharm. Res.* 31 (7) (2014) 1846–1854.
- [8] P. Schipper, K. van der Maaden, S. Romeijn, C. Oomens, G. Kersten, J. Bouwstra, et al., Determination of depth-dependent intradermal immunogenicity of adjuvanted inactivated polio vaccine delivered by microinjections via hollow microneedles, *Pharm. Res.* 33 (9) (2016) 2269–2279.
- [9] P. Schipper, K. van der Maaden, S. Romeijn, C. Oomens, G. Kersten, W. Jiskoot, et al., Repeated fractional intradermal dosing of an inactivated polio vaccine by a single hollow microneedle leads to superior immune responses, *J. Control. Release* (2016).
- [10] L. Zhao, A. Seth, N. Wibowo, C. Zhao, N. Mitter, C. Yu, Nanoparticle vaccines, *Vaccine* 32 (3) (2014) 327–337.
- [11] T. Kundig, T. Storni, T. Kundig, G. Senti, P. Johansen, Immunity in response to particulate antigen-delivery systems, *Adv. Drug Deliv. Rev.* 57 (3) (2005) 333–355.
- [12] S. Parveen, R. Misra, S. Sahoo, Nanoparticles: a boon to drug delivery, therapeutics, diagnostics and imaging, *Nanomedicine* 8 (2) (2012) 147–166.
- [13] B. De Geest, M. Willart, H. Hammad, B. Lambrecht, C. Pollard, P. Bogaert, et al., Polymeric multilayer capsule-mediated vaccination induces protective immunity against cancer and viral infection, *ACS Nano* 6 (3) (2012) 2136–2149.
- [14] V. Manolova, A. Flace, M. Bauer, K. Schwarz, P. Saudan, M. Bachmann, Nanoparticles target distinct dendritic cell populations according to their size, *Eur. J. Immunol.* 38 (5) (2008) 1404–1413.
- [15] E. Varypataki, A. Silva, C. Barnier Quer, N. Collin, F. Ossendorp, W. Jiskoot, Synthetic long peptide-based vaccine formulations for induction of cell mediated immunity: a comparative study of cationic liposomes and PLGA nanoparticles, *J. Control. Release* 226 (2016) 98–106.
- [16] E. Varypataki, K. van der Maaden, J. Bouwstra, F. Ossendorp, W. Jiskoot, Cationic liposomes loaded with a synthetic long peptide and poly(I:C): a defined adjuvanted vaccine for induction of antigen-specific T cell cytotoxicity, *AAPS J.* 17 (1) (2015) 216–226.
- [17] S. Hamdy, O. Molavi, Z. Ma, A. Haddadi, A. Alshamsan, Z. Gobti, et al., Co-delivery of cancer-associated antigen and Toll-like receptor 4 ligand in PLGA nanoparticles induces potent CD8 + T cell-mediated anti-tumor immunity, *Vaccine* 26 (39) (2008) 5046–5057.
- [18] F. Danhier, E. Ansorena, J. Silva, A. Le Breton, R. Coco, V. Préat, PLGA-based nanoparticles: an overview of biomedical applications, *J. Control. Release* 161 (2) (2012) 505–522.
- [19] J. Panyam, V. Labhasetwar, Biodegradable nanoparticles for drug and gene delivery to cells and tissue, *Adv. Drug Deliv. Rev.* 55 (3) (2003) 329–347.
- [20] J. Panyam, V. Labhasetwar, Biodegradable nanoparticles for drug and gene delivery to cells and tissue, *Adv. Drug Deliv. Rev.* 64 (Supplement) (2012) 61–71.
- [21] C. Chong, Enhancement of T helper type 1 immune responses against hepatitis B virus core antigen by PLGA nanoparticle vaccine delivery, *J. Control. Release* 102 (1) (2005) 85–99.
- [22] E. Schlosser, M. Mueller, S. Fischer, S. Basta, D. Busch, B. Gander, et al., TLR ligands and antigen need to be coencapsulated into the same biodegradable microsphere for the generation of potent cytotoxic T lymphocyte responses, *Vaccine* 26 (13) (2008) 1626–1637.
- [23] T. Akagi, M. Baba, M. Akashi, S. Kunugi, T. Yamaoka, Biodegradable Nanoparticles as Vaccine Adjuvants and Delivery Systems: Regulation of Immune Responses by Nanoparticle-Based Vaccine, Springer Berlin Heidelberg, Berlin, 2012, pp. 31–64.
- [24] M. Zaric, O. Lyubomska, O. Touzelet, C. Poux, S. Al Zahrani, F. Fay, et al., Skin dendritic cell targeting via microneedle arrays laden with antigen-encapsulated poly-D,L-lactide-co-glycolide nanoparticles induces efficient antitumor and antiviral immune responses, *ACS Nano* 7 (3) (2013) 2042–2055.
- [25] B. Slutter, L. Plapied, V. Fievez, M. Alonso Sande, A. des Rieux, B. Slütter, et al., Mechanistic study of the adjuvant effect of biodegradable nanoparticles in mucosal vaccination, *J. Control. Release* 138 (2) (2009) 113–121.
- [26] A.C. Platteel, A.M. de Groot, C. Keller, P. Andersen, H. Ovaa, P. Kloetzel, et al., Strategies to enhance immunogenicity of cDNA vaccine encoded antigens by modulation of antigen processing, *Vaccine* 34 (42) (2016) 5132–5140.
- [27] H. SHEN, M. MATLOUBIAN, R. AHMED, M.K. Slifka, E.R. Jensen, J.F. Miller, Recombinant *Listeria* monocytogenes as a live vaccine vehicle for the induction of protective anti-viral cell-mediated immunity, *Proc. Natl. Acad. Sci. U. S. A.* 92 (9) (1995) 3987–3991.
- [28] C. Pope, S.K. Kim, A. Marzo, D. Masopust, K. Williams, J. Jiang, et al., Organ-specific regulation of the CD8 T cell response to *Listeria monocytogenes* infection, *J. Immunol.* [Internet] 166 (5) (2001) 3402–3409.
- [29] J.M. Kelly, S.J. Sterry, S. Cose, S.J. Turner, J. Fecondo, S. Rodda, et al., Identification of conserved T cell receptor CDR3 residues contacting known exposed peptide side chains from a major histocompatibility complex class I-bound determinant, *Eur. J. Immunol.* 23 (12) (1993) 3318–3326.
- [30] M.J. Barnden, J. Allison, W.R. Heath, F.R. Carbone, Defective TCR expression in transgenic mice constructed using cDNA-based alpha- and beta-chain, *Immunol. Cell Biol.* 76 (1) (1998) 34.
- [31] D.D. McGregor, F.T. Koster, G.B. Mackaness, Biological sciences: the short lived small lymphocyte as a mediator of cellular immunity, *Nature* 228 (1970) 855–856.
- [32] Y. Perrie, A. Mohammed, D. Kirby, S. McNeil, V. Bramwell, Vaccine adjuvant systems: enhancing the efficacy of sub-unit protein antigens, *Int. J. Pharm.* 364 (2) (2008) 272–280.
- [33] J. Silva, M. Videira, V. Preat, H. Florindo, R. Gaspar, V. Préat, Immune system targeting by biodegradable nanoparticles for cancer vaccines, *J. Control. Release* 168 (2) (2013) 179–199.
- [34] H. Shen, A. Ackerman, V. Cody, A. Giodini, E. Hinson, P. Cresswell, et al., Enhanced and prolonged cross-presentation following endosomal escape of exogenous antigens encapsulated in biodegradable nanoparticles, *Immunology* 117 (1) (2006) 78–88.
- [35] Y. Waeckerle Men, E.U. Allmen, B. Gander, E. Scandella, E. Schlosser, G. Schmidtke, et al., Encapsulation of proteins and peptides into biodegradable poly(D,L-lactide-co-glycolide) microspheres prolongs and enhances antigen presentation by human dendritic cells, *Vaccine* 24 (11) (2006) 1847–1857.
- [36] Y. Waeckerle Men, M. Groettrup, PLGA microspheres for improved antigen delivery to dendritic cells as cellular vaccines, *Adv. Drug Deliv. Rev.* 57 (3) (2005) 475–482.
- [37] S. Bal, B. Slutter, W. Jiskoot, J. Bouwstra, B. Slütter, Small is beautiful: N-trimethyl chitosan-ovalbumin conjugates for microneedle-based transcutaneous immunisation, *Vaccine* 29 (23) (2011) 4025–4032.
- [38] A. Kumar, P. Wonganan, M. Sandoval, X. Li, S. Zhu, Z. Cui, Microneedle-mediated transcutaneous immunization with plasmid DNA coated on cationic PLGA nanoparticles, *J. Control. Release* 163 (2) (2012) 230–239.
- [39] H. Ng, G.J.P. Fernando, M.A.F. Kendall, Induction of potent CD8 + T cell responses through the delivery of subunit protein vaccines to skin antigen-presenting cells using densely packed microprojection arrays, *J. Control. Release* 162 (3) (2012) 477–484.
- [40] K. Van Der Maaden, E.M. Varypataki, S. Romeijn, F. Ossendorp, W. Jiskoot, J. Bouwstra, Ovalbumin-coated pH-sensitive microneedle arrays effectively induce ovalbumin-specific antibody and T-cell responses in mice, *Eur. J. Pharm. Biopharm.* 88 (2) (2014) 310–315.
- [41] K. Van Der Maaden, E.M. Varypataki, H. Yu, S. Romeijn, W. Jiskoot, J. Bouwstra, Parameter optimization toward optimal microneedle-based dermal vaccination, *Eur. J. Pharm. Sci.* 64 (2014) 18–25.
- [42] A.D. Bins, A. Jorritsma, M.C. Wolkers, C.F. Hung, Wu TC, T.N.M. Schumacher, et al., A rapid and potent DNA vaccination strategy defined by in vivo monitoring of antigen expression, *Nat. Med.* 11 (8) (2005) 899–904.
- [43] C. Fehres, J. Garcia Vallejo, W.W.J. Unger, Y. van Kooyk, Skin-resident antigen-presenting cells: instruction manual for vaccine development, *Front. Immunol.* 4 (2013) 157.
- [44] M. Zaric, O. Lyubomska, C. Poux, M.L. Hanna, M.T. McCrudden, B. Malissen, et al., Dissolving microneedle delivery of nanoparticle-encapsulated antigen elicits efficient cross-priming and Th1 immune responses by murine Langerhans cells, *J. Invest. Dermatol.* 135 (2) (2015) 425–434.
- [45] W. Weldon, V. Zarnitsyn, E.S. Esser, M. Taherbhai, D. Koutsouanos, E. Vassilieva, et al., Effect of adjuvants on responses to skin immunization by microneedles coated with influenza subunit vaccine, *PLoS One* 7 (7) (2012) e41501.
- [46] C. Foged, B. Brodin, S. Frokjaer, A. Sundblad, Particle size and surface charge affect particle uptake by human dendritic cells in an in vitro model, *Int. J. Pharm.* 298 (2) (2005) 315–322.
- [47] S. Demento, W. Cui, J. Criscione, E. Stern, J. Tulipan, S. Kaech, et al., Role of sustained antigen release from nanoparticle vaccines in shaping the T cell memory phenotype, *Biomaterials* 33 (19) (2012) 4957–4964.
- [48] M. Pihlgren, C. Arpin, T. Walzer, M. Tomkowiak, A. Thomas, J. Marvel, et al., Memory CD44(int) CD8 T cells show increased proliferative responses and IFN-gamma production following antigenic challenge in vitro, *Int. Immunol.* 11 (5) (1999) 699–706.
- [49] A. Roberts, K. Ely, D. Woodland, Differential contributions of central and effector memory T cells to recall responses, *J. Exp. Med.* 202 (1) (2005) 123–133.
- [50] M.M. Opatka, R. Stephens, Early decision: effector and effector memory T cell differentiation in chronic infection, *Curr. Immunol. Rev.* 9 (3) (2013 Aug) 190–206.